

Inhibition of Osteogenic Differentiation of Human Adipose-Derived Stromal Cells by Retinoblastoma Binding Protein 2 Repression of RUNX2-Activated Transcription

WENSHU GE,^a LEI SHI,^b YONGSHENG ZHOU,^a YUNSONG LIU,^a GUI-E MA,^c YONG JIANG,^d
YONGWEI XU,^a XIAO ZHANG,^a HAILAN FENG^a

^aDepartment of Prosthodontics and ^dDepartment of General Dentistry 2, Peking University School and Hospital of Stomatology, Beijing, China; ^bMouse Cancer Genetics Program, Center for Cancer Research, National Cancer Institute, Frederick, Maryland, USA; ^cBody Sculpture Center, Plastic Surgery Hospital, Chinese Academy of Medical Sciences, Beijing, China

Key Words. Human adipose-derived stromal cells • Retinoblastoma binding protein 2 • Histone methylation • RUNX2 • Osteogenic differentiation

ABSTRACT

Histone methylation is regarded as an important type of histone modification defining the epigenetic program during the lineage differentiation of stem cells. A better understanding of this epigenetic mechanism that governs osteogenic differentiation of human adipose-derived stromal cells (hASCs) can improve bone tissue engineering and provide new insights into the modulation of hASC-based cell therapy. Retinoblastoma binding protein 2 (RBP2) is a histone demethylase that specifically catalyzes demethylation of dimethyl or trimethyl histone H3 lysine 4 (H3K4me2 or H3K4me3), which is normally associated with transcriptionally active genes. In this study, the roles of RBP2 in osteogenic differentiation of hASCs were investigated. We found that *RBP2* knockdown by lentiviruses expressing small interfering RNA promoted osteogenic differentiation of hASCs *in vitro* and *in vivo*. In addition, we demonstrated that

knockdown of *RBP2* resulted in marked increases of mRNA expression of osteogenesis-associated genes such as *alkaline phosphatase (ALP)*, *osteocalcin (OC)*, and *osterix (OSX)*. RBP2 was shown to occupy the promoters of *OSX* and *OC* to maintain the level of the H3K4me3 mark by chromatin immunoprecipitation assays. Furthermore, coimmunoprecipitation and luciferase reporter experiments suggested that RBP2 was physically and functionally associated with RUNX2, an essential transcription factor that governed osteoblastic differentiation. Significantly, *RUNX2* knockdown impaired the repressive activity of RBP2 in osteogenic differentiation of hASCs. Altogether, our study is the first to demonstrate the functional and biological roles of H3K4 demethylase RBP2 in osteogenic differentiation of hASCs and to link RBP2 to the transcriptional regulation of RUNX2. *STEM CELLS* 2011;29:1112–1125

Disclosure of potential conflicts of interest is found at the end of this article.

INTRODUCTION

Human adipose-derived stromal cells (hASCs) are a type of adult mesenchymal stem cells capable of self-renewal and differentiation into cells such as osteoblasts, chondrocytes, and adipocytes [1]. When compared with bone marrow-derived mesenchymal stem cells, hASCs can be obtained from adipose tissues that offer a more abundant and accessible pool of mesenchymal stem cells that can be obtained by a less invasive and less expensive procedure [1–4]. Thus, hASCs have become a highly attractive source of adult mesenchymal stem cells in bone tissue engineering and have promising prospects in bone regeneration [2, 3].

How to effectively promote osteogenic differentiation of hASCs then has become a core issue in the bone regeneration or tissue engineering fields. Previous studies focused on modulating the conditions for induction [5–7] or integrating exogenous genes into the original genome (changing the original genome sequence) [8, 9] to facilitate osteogenic differentiation. Recent evidence suggest that epigenetic regulation, heritable changes in the genome independent of the DNA sequence, plays a key role in the fate maintenance and determination of stem cells [10]. It has been demonstrated that the DNA methylation pattern such as CpG hypo- or hyper-methylation, an important epigenetic phenomenon, at lineage-specific promoters functions as a key determinant in epigenetic commitment of hASCs to a specific lineage [11, 12]. However, there have

Author contributions: W. G. and L. S.: study design, collection and assembly of data, data analysis and interpretation, manuscript writing; Y. Z.: leader of the project, conception and design, financial support, data analysis and interpretation, manuscript writing, final approval of manuscript; Y. L.: data analysis and interpretation; G. M.: provision of study material or patients; Y. J. and H. F.: administrative support; Y. X. and X. Z.: collection and assembly of data. W.G. and L.S. contributed equally to this article.

Correspondence: Yongsheng Zhou, D.D.S., Ph.D., Department of Prosthodontics, Peking University School and Hospital of Stomatology, 22 Zhongguancun Nandajie, Haidian District, Beijing 100081, People's Republic of China. Telephone: 86-10-6217-9977, ext. 5370; Fax: 86-10-6217-3402; e-mail: kqzhouysh@hsc.pku.edu.cn Received February 17, 2011; accepted for publication May 1, 2011; first published online in *STEM CELLS EXPRESS* May 20, 2011. © AlphaMed Press 1066-5099/2009/\$30.00/0 doi: 10.1002/stem.663

been few reports on how the histone methylation, another important epigenetic mechanism, contributes to osteogenic differentiation of hASCs.

Histone methylation has been implicated in many biological processes that include heterochromatin formation, genomic imprinting, X-chromosome inactivation, and transcriptional regulation [13]. This type of histone modification is regarded as a major mechanism of epigenetic modulation, especially in the lineage determination and differentiation of stem cells [14, 15]. Recent studies demonstrated that analogous to other histone modifications, such as acetylation, histone methylation is also reversible and can be eliminated by demethylases that act via amine oxidation, hydroxylation, or deimination [16–21]. Retinoblastoma binding protein 2 (RBP2) is one of these histone demethylases that catalyzes the removal of dimethylation and trimethylation at histone H3 lysine 4 (H3K4) and regulates the methylation pattern of histones [22, 23]. Therefore, it would be of interest to clarify its functional roles in fate maintenance and determination of stem cells. Some studies have shown that RBP2 can repress differentiation of embryonic stem cells, which can be counteracted when displaced from Hox genes, correlating with an increase of trimethylated H3K4 (H3K4me3) levels at the promoter regions and activation of these genes [22, 24]. However, the role of RBP2 in osteogenic differentiation of hASCs is not fully understood.

In this study, we investigated the functional role of the H3K4 demethylase RBP2 in osteogenic differentiation of hASCs. Our study is the first to suggest that modification of chromatin structure triggered by RBP2 is critical for osteogenic differentiation of hASCs. Understanding this function will improve our knowledge of the epigenetic mechanisms governing the osteoblastic lineage differentiation of hASCs, which would benefit the development of bone tissue engineering or cell therapy based on hASCs.

MATERIALS AND METHODS

Cell Isolation, Culture, and Osteogenic Induction

Human adipose tissues were obtained with informed consent from five donors with no known medical morbidities between the ages of 22 and 27 years with an average body mass index of 24. These subjects were undergoing liposuction surgery for esthetic reasons at the plastic surgery hospital affiliated with the Chinese Academy of Medical Science. The study was approved by the Ethics Committee of the Peking University Health Science Center, Beijing, China. hASCs were isolated and cultured according to our previously published articles [7]. Cells of the third passage were used for the *in vitro* experiments, which were repeated three times using hASCs from three of the patients. Cells of the fourth passage from the other two patients were used for the *in vivo* experiments. Osteogenic differentiation was induced with Dulbecco's modified Eagle medium (DMEM) containing 10% fetal bovine serum, 100 IU/ml penicillin/streptomycin, 100 nM dexamethasone, 0.2 mM ascorbic acid, and 10 mM β -glycerophosphate.

Plasmid Constructions

Wild-type human *RBP2* (Wt *RBP2*) was subcloned from pcDNA3-HA-*RBP2* [23, 25] into the pcDNA3.1-3 \times FLAG vector between the *NotI* and *XbaI* sites. The mutant demethylase *RBP2* (Mt *RBP2*) was generated from pcDNA3.1-3FLAG-Wt *RBP2* by using the Quikchange Site-Directed Mutagenesis Kit (Stratagene, Santa Clara, CA, www.genomics.agilent.com) and the primers: 5'-ttttgctggGCTattgagatc-3' (forward) and 5'-gatcctcaatAGCccagcaaaa-3' (reverse). Mouse *RUNX2* was subcloned from pCMV2-FLAG-*RUNX2* into the

pcDNA3.1(+)-Myc-His vector between the *EcoRV* and *XbaI* sites. GST-*RUNX2* was subcloned from pCMV2-FLAG-*RUNX2* into the pGEX4T3 vector between the *SalI* and *XhoI* sites using the primers: (forward) 5'-GTCGGCCATAACGCGTGCACCTTCATTTCGCCTCACAAAC-3' and (reverse) 5'-CCGCTCGAGTCAATATGGTCGCCAAACAG-3'.

RNA Interference and Lentiviral Production and Infection

Small interfering RNA (siRNA) sequences targeting *RBP2* (siRNA-1: GCTGTACGAGAGTATACAC, siRNA-2: GGCGGACGTTTCTTAAGAA), *RUNX1* (GGCAGAACTA-GATGATCA), or *RUNX2* (GGTTCAACGATCTGAGATT) were designed and cloned into the pLL3.7 shuttle vector with an independent enhanced green fluorescent protein (EGFP) cassette. The recombinant construct and nonspecific siRNA construct (control group) as well as three helper vectors (pMDLg/pRRE, pRSV-REV, and pVSVG) were then transiently transfected into HEK293T cells. The viral supernatants were collected 48 hours later, clarified by filtration, and concentrated by ultracentrifugation. The concentrated viruses were used to infect hASCs. The infected cells were then induced to become osteoblasts, and the differences in osteogenic differentiation between the knockdown group and control group were compared.

ALP Activity of hASCs

The hASCs were seeded in six-well plates, and alkaline phosphatase (ALP) activity was determined by staining with nitro blue tetrazolium and 5-bromo-4-chloro-3-indolyl phosphate on the 14th day after osteogenic differentiation. For quantification of ALP activity, cells seeded in six-well plates were rinsed two times with phosphate-buffered saline (PBS), followed by trypsinization, and then scraping in ddH₂O. This was followed by three cycles of freezing and thawing. ALP activity was determined at 405 nm using *p*-nitrophenyl phosphate (pNPP) as the substrate. A 50- μ l sample was mixed with 50 μ l pNPP (1 mg/ml) in 1 M diethanolamine buffer containing 0.5 mM MgCl₂ (pH 9.8) and incubated at 37°C for 15 minutes on a bench shaker. The reaction was stopped by the addition of 25 μ l of 3 M NaOH/100 μ l of reaction mixture. Enzyme activities were quantified by absorbance measurements at 405 nm. Total protein contents were determined with the bicinchoninic acid method using the Pierce (Thermo Fisher Scientific, Rockford, IL, www.piercenet.com) protein assay kit in aliquots of the same samples, which were read at 562 nm and calculated against a series of bovine serum albumin (BSA) standards. ALP levels were normalized to the total protein content at the end of the experiment.

Mineralization Assays for hASCs

The hASCs were seeded in six-well plates, and mineralization was determined by staining with alizarin red S on days 7 and 14 after osteogenic differentiation. To quantify matrix mineralization, alizarin red S-stained cultures were incubated in 100 mM cetylpyridinium chloride for 1 hour to solubilize and release calcium-bound alizarin red S into the solution. The absorbance of the released alizarin red S was measured at 562 nm. Data were expressed as units of alizarin red S released (1 unit = 1 unit of optical density at 562 nm) per milligram of protein in each culture in a parallel well. This test was repeated three times.

In Vivo Implantation of hASCs and Bio-Oss Collagen Scaffold Hybrids

hASCs were induced by osteogenic medium or cultured in proliferation medium for 1 week before the *in vivo* study.

hASCs (1×10^6 cells) were resuspended directly into DMEM and then seeded on the Bio-Oss Collagen (Geistlich, GEWO GmbH, Baden-Baden, Germany, www.osteohhealth.com) scaffolds. hASCs were divided into four groups: (a) *RBP2*-RNAi (siRNA-2) hASCs induced by osteogenic medium; (b) *RBP2*-RNAi (siRNA-2) hASCs cultured in proliferation medium; (c) control hASCs induced by osteogenic medium; (d) control hASCs cultured in proliferation medium. For in vivo evaluations, 4 to 6-week-old BALB/c homozygous nude (nu/nu) mice were used (Peking University Experimental Animal Center). hASCs-seeded scaffolds were implanted into the dorsal subcutaneous space of the mice ($n = 5$ per group). All animal experiments were performed in accordance with the institutional animal guidelines.

Analyses of Bone Formation In Vivo

Specimens of each group were harvested at 6 weeks after implantation, and animals in each group were sacrificed by CO₂ asphyxiation. X-ray examinations were used to evaluate the mineral density. The bone constructs were fixed in 4% paraformaldehyde and then decalcified for 10 days in 10% EDTA (pH 7.4). After decalcification, the specimens were dehydrated and subsequently embedded in paraffin. Sections (5 mm thickness) were stained with H&E and Masson's trichrome. Osteogenesis was evaluated with immunohistochemical analysis for osteopontin (OPN) and osteocalcin (OC) (sp kit, Vector, Burlingame, CA, www.vectorlabs.com, primary antibody was purchased from Santa Cruz Biotechnology, Santa Cruz, CA, www.scbt.com). Specimens were processed using identical protocols.

RNA Extraction, Reverse Transcription, and Quantitative RT-PCR

Total cellular RNAs were isolated with Trizol reagent (Invitrogen, Carlsbad, CA, www.invitrogen.com) and used for first strand cDNA synthesis with the Reverse Transcription System (Promega, Madison, WI, www.promega.com). Quantifications of all gene transcripts were performed by real-time polymerase chain reaction (RT-PCR) using a Power SYBR Green PCR Master Mix and an ABI PRISM 7300 sequence detection system (Applied Biosystems, Foster City, CA, www.appliedbiosystems.com) with the expression of *GAPDH* detected as the internal control. The primers used were: *ALP*, (forward) 5'-ATGGGATGGGTGTCTCCACA-3' and (reverse) 5'-CCACGAAGGGAACTTGTG-3'; *OC*, (forward) 5'-CACTCCTCGCCATTGGC-3' and (reverse) 5'-CCCTCCTGCTGGACACAAAG-3'; *OSX*, (forward) 5'-CCTCTGCGGGACTCAAAC-3' and (reverse) 5'-TAAAGGGGGCTGGATAAGCAT-3'; and *RBP2*, (forward) 5'-GTCCAGCGCCTGAATGACTT-3' and (reverse) 5'-GCAACAATCTTGCTCAAAGCATA-3'. The cycle threshold values (Ct values) were used to calculate the fold differences by the $\Delta\Delta C_t$ method.

ChIP Assay

The chromatin immunoprecipitation (ChIP) assay was performed as previously described [26, 27]. Briefly, hASCs were cross-linked in 1% formaldehyde at 37°C for 10 minutes and resuspended in 200 μ l lysis buffer (1% sodium dodecyl sulfate [SDS], 10 mM EDTA, and 50 mM Tris-HCl [pH 8.1]) and the nuclear lysates were sonicated and diluted 10-fold with immunoprecipitation buffer (16.7 mM Tris-HCl, pH 8.1; 167 mM NaCl; 1.2 mM EDTA; 0.01% SDS; and 1.1% Triton X-100). The lysates were then immunoprecipitated with non-specific rabbit IgG, H3K4me3, H3K9me3, RBP2, or H3 antibodies (all from Abcam, Cambridge, MA, www.abcam.com) for 12 hours at 4°C. Immune complexes were incubated with Protein G-Sepharose CL-4B (GE Healthcare, Piscataway, NJ, www.gehealthcare.com) for 2 hours at 4°C. After successive

washings, immune complexes containing DNA were purified and eluted, and the precipitated DNA was amplified by PCR. Primer pairs used in this study were as follows: *OC* promoter, (forward) 5'-GTGGCTCACCTCCATCAC-3' and (reverse) 5'-CCTCCAGCACTGTTTATACCCT-3' and *OSX* promoter, (forward) 5'-AGCAGCAGTAGCAGAAGCA-3' and (reverse) 5'-CAGCAGTCCCATAGGCATC-3'.

Co-Immunoprecipitation

Saos-2 or HEK293 cell lysates were prepared by incubating the cells in lysis buffer (50 mM Tris-HCl, pH 8.0, 150 mM NaCl, 0.1% Nonidet P-40) for 20 minutes at 4°C. This was followed by centrifugation at 14,000g for 15 minutes at 4°C. For immunoprecipitation, 500 μ g of protein were incubated with specific antibodies (2 μ g) for 12 hours at 4°C with constant rotation. Fifty microliters of 50% protein A or G agarose beads was then added, and the incubation was continued for an additional 2 hours. Beads were then washed five times in lysis buffer. Between washes, the beads were collected by centrifugation at 3,000g for 30 seconds at 4°C. The precipitated proteins were eluted from the beads by resuspension in 2 \times SDS-polyacrylamide gel electrophoresis (SDS-PAGE) loading buffer and boiling for 5 minutes. The boiled immune complexes were analyzed by SDS-PAGE, followed by immunoblotting with appropriate antibodies with an input of 5%.

Reporter Assay

For luciferase assays, HEK293 cells were cultured in 12-well plates for 1 day before transfection. *RUNX2*, p*OC*-luc, Wt *RBP2*, or Mt *RBP2* constructs were transiently transfected using Lipofectamine 2000 (Invitrogen) according to the manufacturer's instructions. At 36 hours post-transfection, cell lysates were analyzed for luciferase activity using the Dual-Luciferase Reporter Assay kit (Promega) according to the manufacturer's protocol. Each experiment was performed in triplicate and repeated at least three times.

GST Pull-Down Assay

GST fusion proteins were expressed in BL21 cells. After induction with 1 mM isopropyl- β -thiogalactopyranoside (3 hours, 30°C), the cells were sonicated in PBS containing 1% Triton X-100. For the GST pull-down assay, 1–2 μ g GST-RUNX2 protein was coupled to 100 μ l glutathione-sepharose 4B (GE Healthcare). The matrix was incubated with in vitro transcribed and translated RBP2 overnight at 4°C. After extensive washing, bound proteins were eluted by boiling in 2 \times Laemmli buffer, resolved on a 8% SDS-PAGE, and analyzed by Western blotting.

RESULTS

RBP2 Inhibits Osteogenic Differentiation of hASCs In Vitro

To characterize the role of RBP2 in osteogenic differentiation of hASCs, we depleted *RBP2* expression in hASCs by using lentiviral vectors expressing siRNA. Two siRNA sequences against *RBP2* were designed, and the corresponding DNA was inserted into the pLentilox vector, followed by lentiviral packaging. After infection of hASCs, the lentiviruses expressing siRNA against *RBP2* dramatically decreased the expression level of *RBP2*, regardless of whether the cells were induced to differentiate or not (Fig. 1A). The activity of ALP was accelerated in *RBP2*-depleted hASCs when compared with control siRNA treated cells when cultured in osteogenic medium for the indicated periods (Fig. 1B). Furthermore, the extracellular matrix mineralization, as shown by alizarin red S staining and

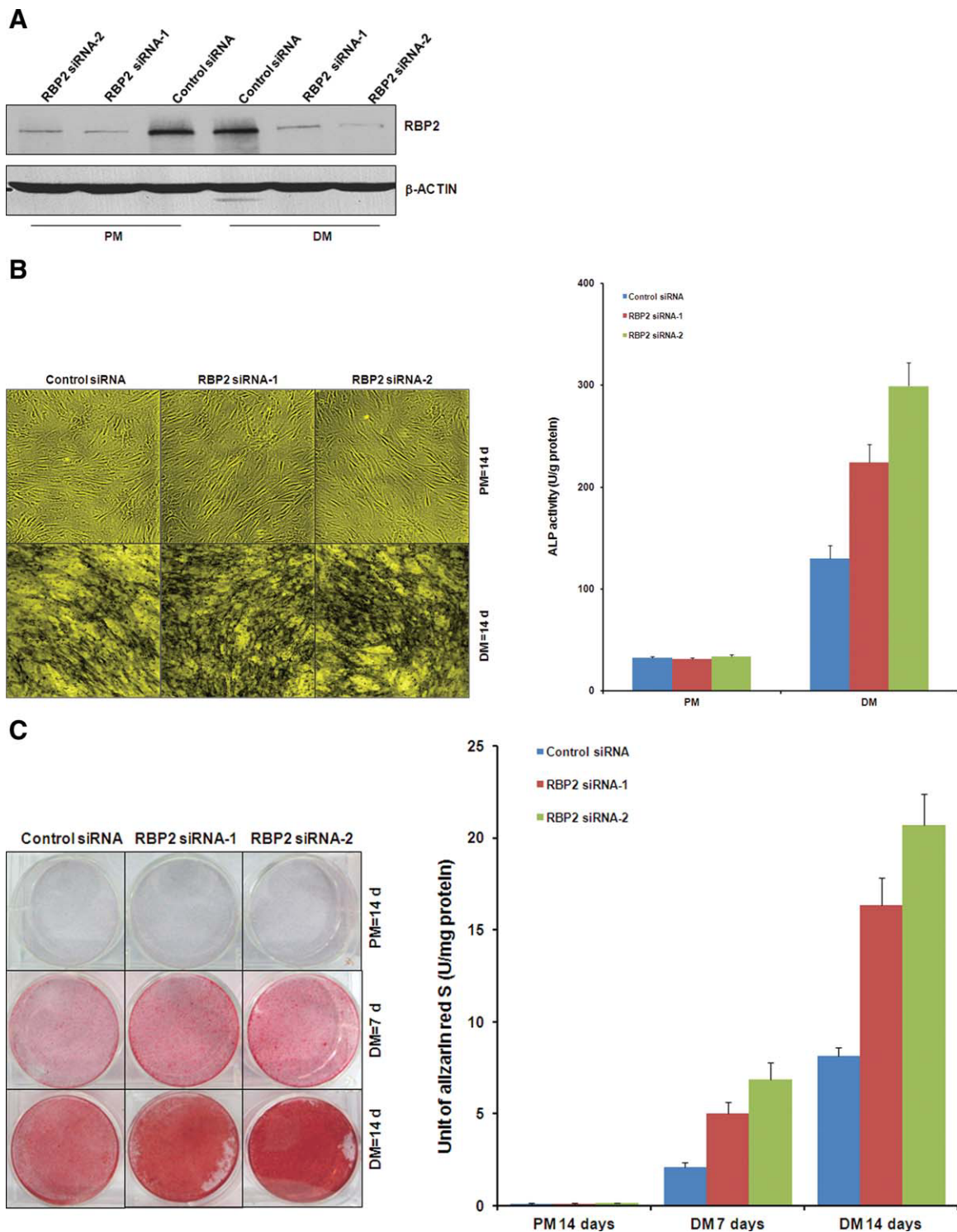


Figure 1. Retinoblastoma binding protein 2 (RBP2) loss of function promotes osteogenic differentiation of human adipose-derived stromal cells (hASCs) in vitro. **(A):** The *RBP2* knockdown effect was validated by Western blotting. hASCs infected with lentivirus expressing control or *RBP2* siRNA were cultured in proliferation or differentiation medium for 7 days. Cellular lysates were immunoblotted with antibodies against the indicated proteins. β -Actin was detected as a loading control. **(B):** *RBP2* knockdown increased alkaline phosphatase (ALP) activity in hASCs. Control or *RBP2* knockdown hASCs were treated with proliferation or differentiation media for 14 days for ALP staining (left panel), and cellular extracts were prepared to quantify ALP activity (right panel). Each bar represents the mean \pm SD for triplicate experiments. **(C):** *RBP2* knockdown promoted matrix mineralization in hASCs. Cells were treated with proliferation or differentiation media with or without *RBP2* knockdown for 7 and 14 days, and then calcium deposition was observed using alizarin red S staining (left panel) and quantification (right panel). Abbreviations: ALP, alkaline phosphatase; DM, osteogenic differentiation medium; PM, proliferation medium; RBP2, retinoblastoma binding protein 2; siRNA, small interfering RNA.

quantification, was also accelerated in *RBP2* siRNA treated cells when compared with control siRNA treated cells (Fig. 1C). Taken together, these results indicated that *RBP2* knockdown in hASCs promoted osteogenic differentiation in vitro.

RBP2 Suppression Stimulates Osteogenic Differentiation of hASCs In Vivo

To further investigate the role of RBP2 in osteogenic differentiation of hASCs, hASCs treated in four different conditions were seeded in Bio-Oss Collagen scaffolds, and the hASC-scaffold hybrids were implanted into the subcutaneous tissue of nude mice. The implanted hASCs cultured in proliferation medium or osteogenic differentiation medium had either unchanged expression of *RBP2* (infected with lentivirus expressing control siRNA) or specific knockdown of *RBP2* expression (infected with lentivirus expressing *RBP2* siRNA). Six weeks after implantation, subcutaneous masses with relatively hard texture were detected, and the hASC-scaffold hybrids were harvested. When mineralization of these hybrids was monitored by x-ray radiography in vitro, we found that pretreatment in differentiation medium stimulated more obvious mineralization over the 6 weeks following implantation of hASC-scaffold hybrids when compared with the proliferation medium alone (Fig. 2A). After the induction of differentiation, hybrids containing hASCs with *RBP2* knockdown showed more mineralization than hybrids containing hASCs without *RBP2* knockdown (Fig. 2A). Furthermore, histological examination corroborated the findings from the x-ray radiography (Fig. 2B, 2C). The spotty areas of osteoid and bone matrix formation were examined by H&E and Masson's trichrome staining, respectively. Consistent with the observations from x-ray radiography, the osteogenic differentiation potential was markedly increased for hybrids containing hASCs with *RBP2* knockdown when compared with those without *RBP2* knockdown (Fig. 2B, 2C). Meanwhile, immunohistochemistry staining showed that the osteogenic markers OPN and OC were highly induced in the hybrids containing hASCs preinduced in osteogenic medium (Fig. 2D, 2E). Notably, this effect was also mildly enhanced by *RBP2* knockdown (Fig. 2D, 2E). To figure out whether the newly formed bone was from the actual cells implanted or not, we checked the GFP signals released from lentivirus-infected hASCs by fluorescence microscope. We found that the bone-forming cells still showed obvious GFP signals (Supporting Information Fig. 1). Taken together, these results substantiated the concept that RBP2 could inhibit osteogenic differentiation of hASCs in vivo.

RBP2 Inhibits the Expression of Osteogenesis-Associated Genes

The observation that *RBP2* depletion resulted in acceleration of osteogenic differentiation of hASCs prompted us to further test whether this effect resulted from the changes in expression of osteogenesis-associated genes. Therefore, we compared the expression of osteogenesis-associated genes, such as *ALP*, *OC*, and *OSX* (also known as *SP7*), between the *RBP2* knockdown hASCs and control hASCs in response to osteogenic stimulation for 14 days by RT-PCR analyses (Fig. 3A–3C). When compared with the control siRNA lentivirus treated hASCs, knockdown of *RBP2* resulted in a marked increase in the mRNA expression levels of *ALP*, *OC*, and *OSX*, although to variable extents (Fig. 3A–3C), which further supported our hypothesis that acceleration of osteogenic differentiation in *RBP2* depleted cells was due to increased expression of these genes. *RBP2* knockdown effects in this experiment were examined by RT-PCR and shown in

Figure 3D. These observations indicated that RBP2 could inhibit the expression of osteogenesis-associated genes.

RBP2 Governs the H3K4me3 Level on Promoters of Osteogenesis-Associated Genes

To gain further insight into the physiological role of RBP2 during osteogenic differentiation of hASCs and to test whether RBP2 was directly involved in the regulation of osteogenesis-associated genes, we examined the recruitment of RBP2 on *OSX* and *OC* promoters in vivo. ChIP assays were performed in native (uninduced) or osteogenically induced hASCs. These experiments revealed that RBP2 was recruited to the promoters of *OSX* and *OC* but not to that of *GAPDH* in native hASCs (Fig. 4A). Surprisingly, we found that RBP2 enrichment decreased dramatically upon osteogenic induction (Fig. 4B). In addition, this diminishment of RBP2 occupancy was specifically and negatively correlated with increased levels of H3K4me3, which are linked with transcriptionally active chromatin, whereas there were no changes in the levels of histone H3 and H3K9me3 (Fig. 4B). As stated before, RBP2 has been demonstrated to demethylate H3K4me3 in mammalian cells. In light of our observation that RBP2 influenced the expression of osteogenesis-associated genes and its binding negatively correlated with H3K4me3, it is logical to postulate that RBP2 may function to erase the H3K4me3 mark in the regulatory region of osteogenesis-associated genes. To test this hypothesis, the levels of H3K4me3 at the promoters of osteogenesis-associated genes were examined in hASCs with *RBP2* knockdown upon osteogenic induction. As shown in Figure 4C, upon osteogenic induction, the transcriptional activations of *OSX* and *OC* were associated with marked increases in the levels of H3K4me3 on the promoters of these genes. Notably, when compared with control lentivirus-infected cells, cells with loss-of-function of *RBP2* displayed increased amounts of H3K4me3 on the *OSX* and *OC* promoters upon osteogenic induction, especially at day 7, while the total histone H3 levels were not affected (Fig. 4C). However, in proliferation medium, the H3K4me3 mark remained at constantly low levels regardless of whether *RBP2* was knocked down or not (Fig. 4C). Collectively, these data supported the notion that RBP2 occupied *OSX* and *OC* promoters to maintain the levels of H3K4me3.

RBP2 Interacts with RUNX2 and Regulates Its Transcriptional Activity

To further explore the underlying mechanism of RBP2-mediated inhibition of osteogenic differentiation of hASCs, we investigated the physical association between RBP2 and RUNX2, a master regulator of osteogenesis, by co-immunoprecipitation (co-IP) experiments. First, we cotransfected FLAG-tagged *RBP2* and Myc-tagged *RUNX2* into HEK293 cells. Immunoprecipitation with antibodies against FLAG followed by immunoblotting with antibodies against Myc demonstrated that FLAG-RBP2 was co-immunoprecipitated with Myc-RUNX2 (Fig. 5A). To further confirm the in vivo interaction between RBP2 and RUNX2, endogenous co-IP experiments were performed with Saos-2 cell extracts. Immunoprecipitation with antibodies against RBP2 followed by immunoblotting with antibodies against RUNX2 demonstrated that RBP2 was co-immunoprecipitated with RUNX2 but not with β -actin (Fig. 5B, left panel). Reciprocally, immunoprecipitation with antibodies against RUNX2 and immunoblotting with antibodies against RBP2 also revealed that RUNX2 was co-immunoprecipitated with RBP2 but not with β -actin (Fig. 5B, right panel). To further validate the in vivo interaction between RBP2 and RUNX2, protein fractionation experiments

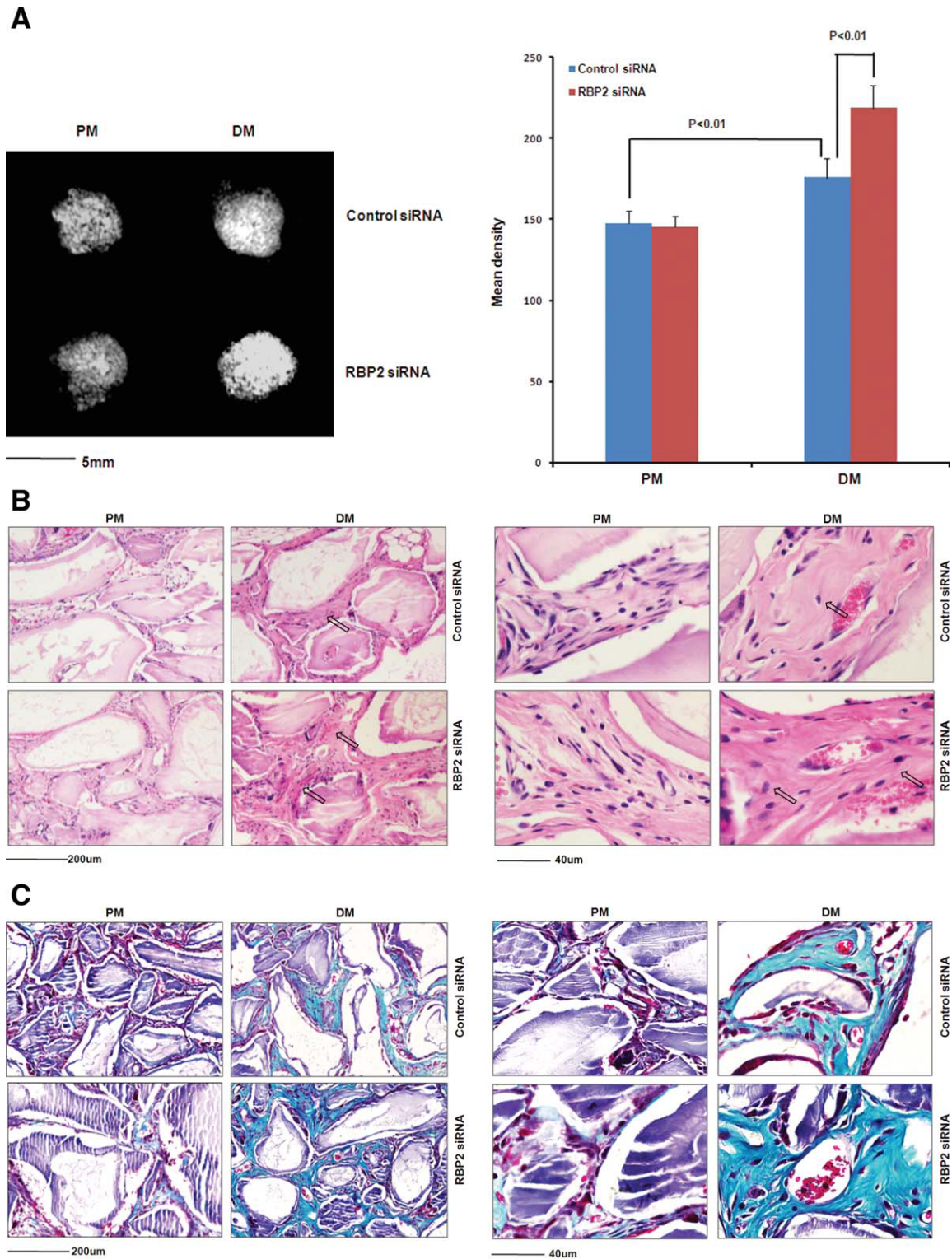


Figure 2. Retinoblastoma binding protein 2 (RBP2) loss of function promotes osteogenic differentiation of human adipose-derived stromal cells (hASCs) in vivo. hASCs treated with control or *RBP2* siRNA were cultured in osteogenic differentiation medium or proliferation medium for 1 week before implantation into nude mice. Specimens of each group were harvested at 6 weeks after implantation. **(A):** Left panel: x-ray radiography of hASC-scaffold complex implanted into nude mice for 6 weeks. Right panel: Relative gray-scale of hASC-scaffold complex determined by Image J software. *p* values were determined by using Student's *t* test. **(B):** H&E staining of histological sections from implanted hASC-scaffold hybrids. Bone structures are marked with black arrows. **(C):** Masson's trichrome staining of histological sections from implanted hASC-scaffold hybrids. Regenerated bone is stained green. **(D):** Immunohistochemistry of osteocalcin in histological sections from implanted hASC-scaffold hybrids. Dark-brown granules indicating positive staining are marked by black arrows. **(E):** Immunohistochemistry of osteopontin in histological sections from implanted hASC-scaffold hybrids. Dark-brown granules indicating positive staining are marked by black arrows. Low magnification images are provided in the left panel, whereas higher magnification images are in the right panels **(B–E)**. Abbreviations: DM, osteogenic differentiation medium; OPN, osteopontin; PM, proliferation medium; RBP2, retinoblastoma binding protein 2; siRNA, small interfering RNA.

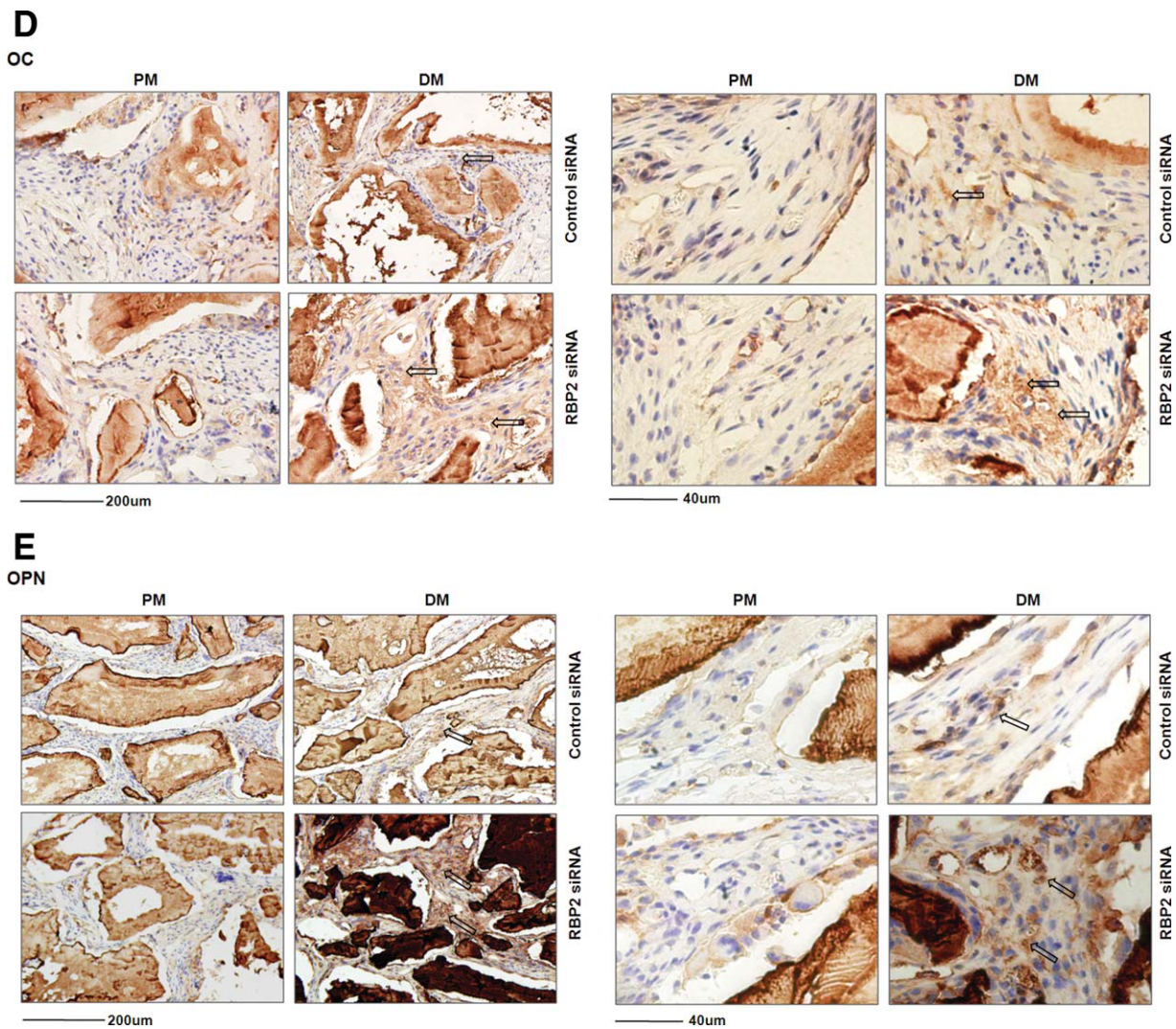


Figure 2. Continued

were carried out by fast protein liquid chromatography with Superose 6 columns and a high salt extraction and size exclusion approach. The results indicated that the elution pattern of RBP2 largely overlapped with that of RUNX2 (Fig. 5C). To determine whether RBP2 was able to interact with RUNX2 directly, *in vitro* GST pull-down experiments were performed with GST-fused full-length RUNX2 and *in vitro* transcribed/translated full-length RBP2 (Fig. 5D). These experiments indicated that RUNX2 directly interacted with RBP2 but not with another “Jumonji C (JmjC) domain” containing histone demethylase JMJD2B. Collectively, these results suggested that RBP2 was physically associated with RUNX2 *in vivo* and *in vitro*.

The physical interaction between RBP2 and RUNX2 suggested that RBP2 may play a role in RUNX2-regulated gene transcriptional activity. To investigate this hypothesis, HEK293 cells were cotransfected with the pOC-luc reporter, RUNX2, and either the Wt RBP2 or demethylase activity defective Mt RBP2 [28, 29]. As shown in Figure 5E, overexpression of RUNX2 resulted in a marked increase of luciferase reporter activity. Furthermore, when compared with the control transfection group, gain of RBP2 function significantly inhibited RUNX2 transcriptional activity, while Mt RBP2 failed to do so. Taken together, these results supported the

notion that RBP2 could functionally repress RUNX2 transcriptional activity through its H3K4 demethylase activity.

Inhibition of Osteogenic Differentiation of hASCs by RBP2 Is Dependent on RUNX2

To further investigate the functional and biological link between RBP2 and RUNX2, we assessed the effect of RUNX2 depletion on RBP2 knockdown hASCs after osteogenic induction for 14 days. For this purpose, RBP2 knockdown hASCs were infected with either lentivirus expressing control siRNA or RUNX2 siRNA. ChIP experiments demonstrated that the bindings of RBP2 to the promoters of OC and OSX were significantly reduced in RUNX2 depleted cells (Fig. 6A), which suggested that in the normal state RBP2 was recruited by RUNX2 to OC and OSX promoters. Consistent with the previous observations, RBP2 knockdown resulted in marked increases in expression of osteogenesis-associated genes. However, RUNX2 depletion greatly impaired this effect (Fig. 6B). Furthermore, the RUNX2 depletion reversed the increase of ALP activity resulting from RBP2 knockdown (Fig. 6C). Moreover, loss of RUNX1 function had no such effect, which suggested that the genetic association between RUNX2 and RBP2 was

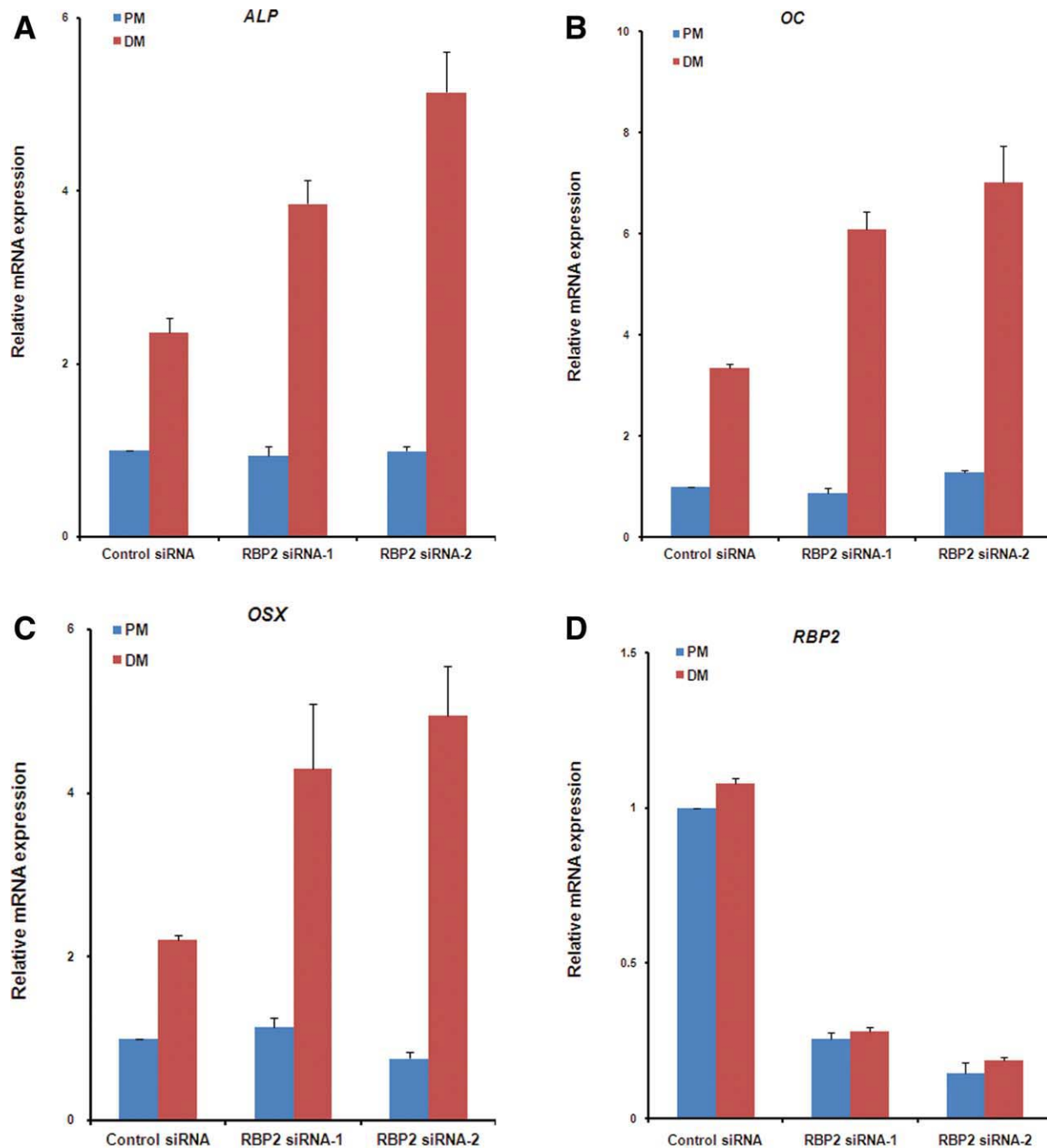


Figure 3. Retinoblastoma binding protein 2 (RBP2) loss of function results in increased expression of osteogenesis-associated genes. (A–C): Human adipose-derived stromal cells were infected with control or *RBP2* siRNA lentiviruses and then cultured in proliferation or differentiation media for 14 days. Total RNAs were extracted from the cells for measurement of the mRNA expression of *alkaline phosphatase (ALP)*, *osteocalcin (OC)*, and *osterix (OSX)* by real-time polymerase chain reaction with the expression of *GAPDH* as a normalizer. (D): Relative *RBP2* mRNA levels were measured to verify the knockdown effects. Each bar represents the mean \pm SD of triplicate experiments. Abbreviations: *ALP*, alkaline phosphatase; DM, osteogenic differentiation medium; *OC*, osteocalcin; *OSX*, osterix; PM, proliferation medium; *RBP2*, retinoblastoma binding protein 2; siRNA, small interfering RNA.

specific (Fig. 6A–6C). In addition, we found that the osteogenic differentiation potential of hASCs was greatly impaired by loss of function of *RUNX2* but not by that of *RUNX1* (Fig. 6B, 6C). The efficiency and specificity of *RBP2*, *RUNX1*, and *RUNX2* knockdown effects in this experiment were confirmed by RT-PCR (Fig. 6D). All together, these results not only substantiated that *RUNX2* functioned as a critical player in osteogenic differentiation of hASCs but also revealed that *RBP2* exerted inhibition of

osteogenic differentiation by physically and genetically repressing the transcriptional activity of *RUNX2*.

DISCUSSION

Our experiments provide the first evidence that histone demethylase *RBP2* physically and functionally interacts with

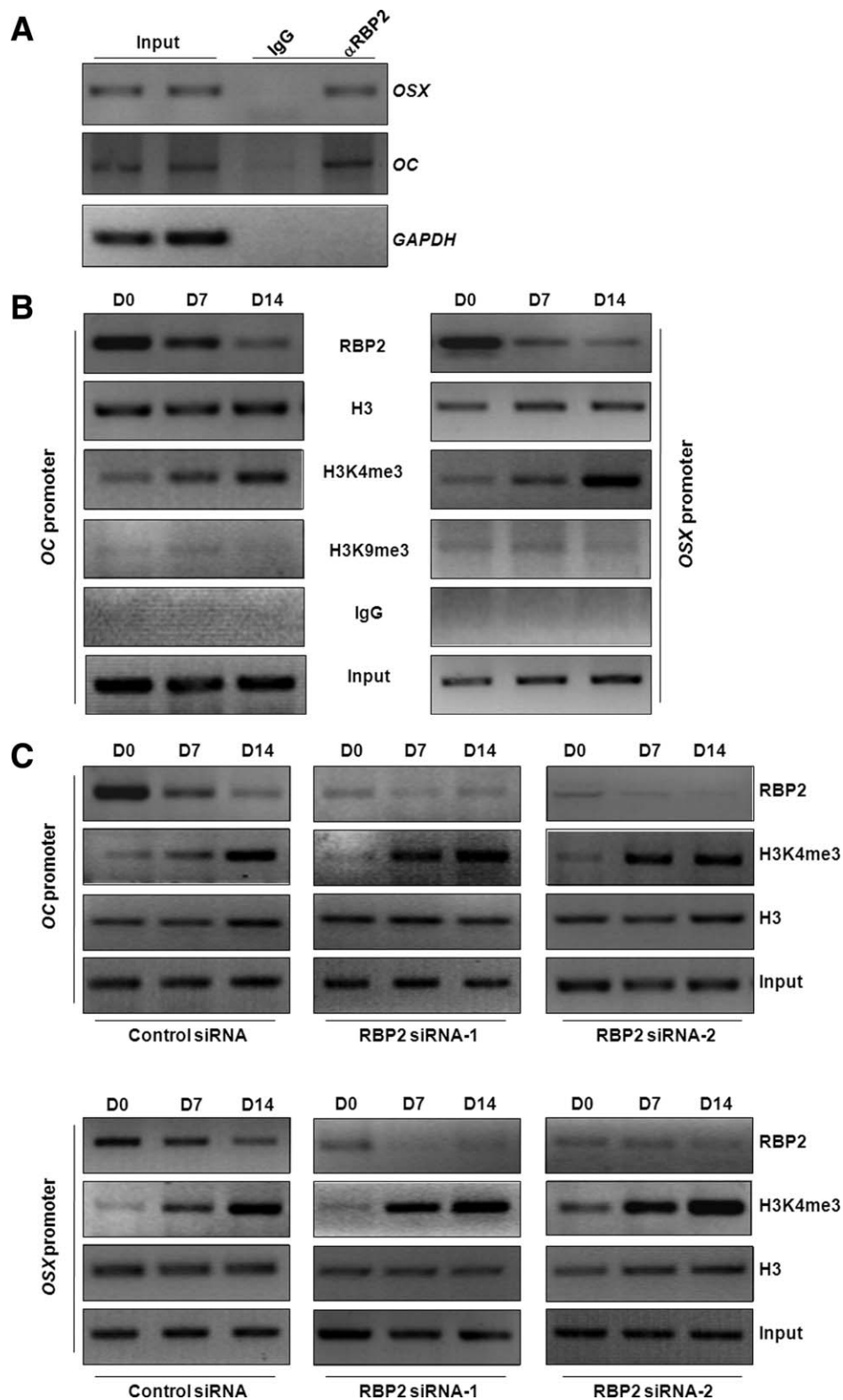


Figure 4. Retinoblastoma binding protein 2 (RBP2) controls the H3K4me3 status at the promoters of osteogenesis-associated genes. (A): RBP2 binds to osteogenesis-associated genes *osterix* (*OSX*) and *osteocalcin* (*OC*) promoters. Soluble chromatin from native human adipose-derived stromal cells (hASCs) were prepared, and chromatin immunoprecipitation (ChIP) assays were performed with antibodies against the indicated proteins. *GAPDH* was used as a negative control. (B): RBP2 occupancy negatively correlated with the H3K4me3 level. Soluble chromatin from native or differentiated hASCs were prepared, and ChIP assays were performed with antibodies against the indicated proteins or histone marks. The cells were cultured in differentiation medium for 7 or 14 days. (C): The effect of *RBP2* knockdown on H3K4 trimethylation of the *OSX* and *OC* promoters. hASCs were treated with control siRNA or *RBP2* siRNA lentivirus and then cultured in differentiation medium for 7 or 14 days. Soluble chromatin was prepared for ChIP assays using the indicated antibodies. Abbreviations: *OC*, *osteocalcin*; *OSX*, *osterix*; RBP2, retinoblastoma binding protein 2; siRNA, small interfering RNA.

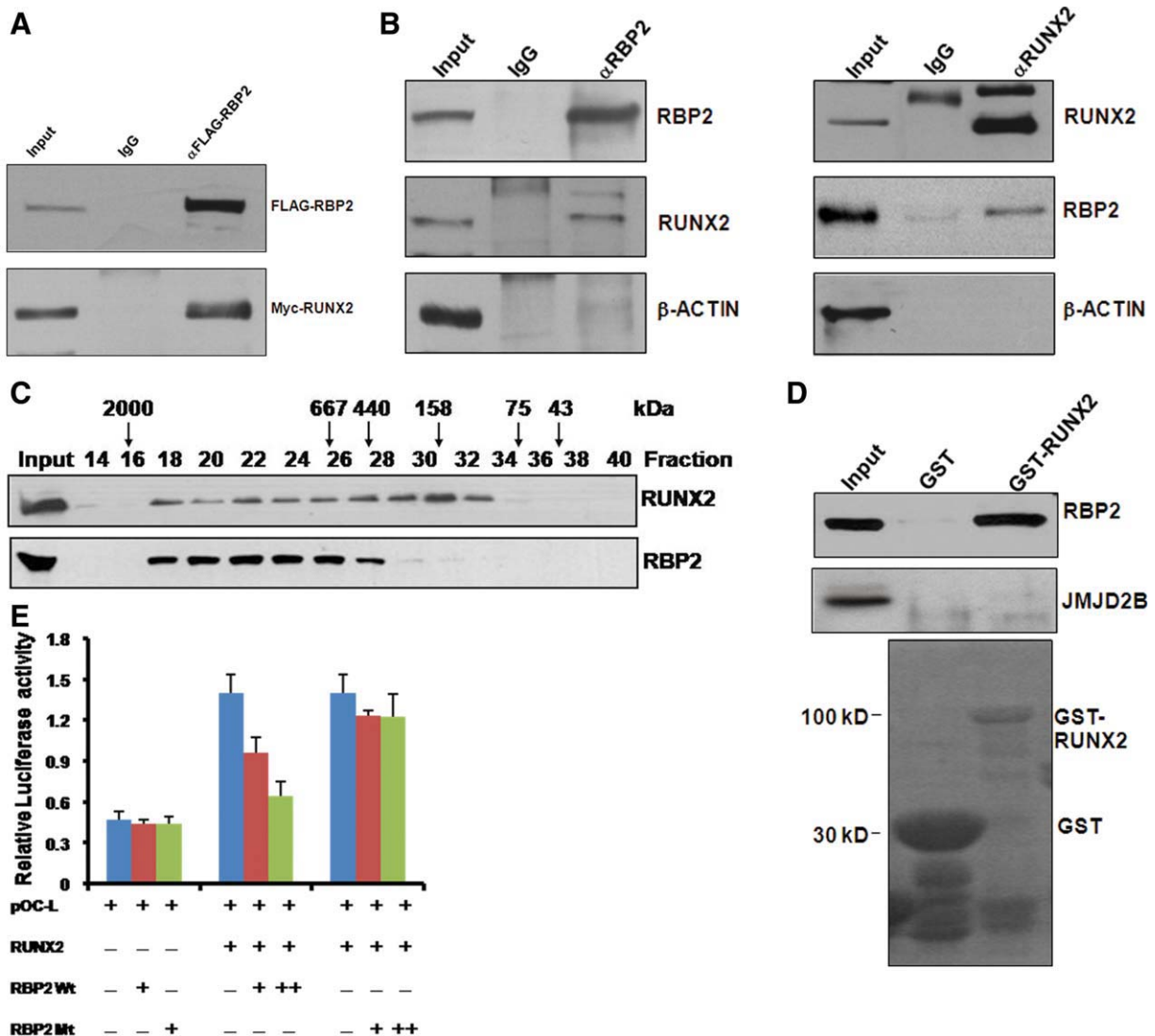


Figure 5. Physical and functional interaction between retinoblastoma binding protein 2 (RBP2) and RUNX2. (A): Exogenous association of RBP2 with RUNX2. Myc-tagged *RUNX2* and FLAG-tagged *RBP2* were cotransfected in HEK293 cells. After immunoprecipitation with anti-FLAG antibodies (α -FLAG), the samples were resolved by SDS-PAGE, and the presence of RUNX2 in the immune complexes was detected with anti-Myc antibodies. The input was 5% of total protein used in the immunoprecipitation experiment. (B): Endogenous association of RBP2 with RUNX2. Whole cell lysates from Saos-2 cells were immunoprecipitated with antibodies against the indicated proteins. Immunocomplexes were then immunoblotted using antibodies against the indicated proteins. β -Actin was used as a negative control. The input was 5% of total protein used in the immunoprecipitation experiment. (C): Cofractionation of protein complexes by fast protein liquid chromatography. Nuclear extracts from Saos-2 cells were fractionated on Superose 6 size exclusion columns. Chromatographic elution profiles and immunoblotting analysis of the chromatographic fractions are shown. The elution positions of calibration proteins with known molecular masses (kDa) are indicated, and an equal volume from each fraction was analyzed. (D): In vitro association between RBP2 and RUNX2 was determined by GST pull-down experiments with bacterially expressed GST-RUNX2 and in vitro transcribed/translated RBP2 or JMJD2B. In vitro purified GST and GST-RUNX2 proteins were detected by Coomassie Blue staining. (E): Regulation of transcriptional activity of RUNX2 by RBP2. HEK293 cells were cotransfected with pOC-luc reporter, *RUNX2*, and wild-type human *RBP2* or mutant demethylase *RBP2*. Cellular extracts were then prepared for reporter assays 36 hours after transfections. Each bar represents the mean \pm SD of triplicate experiments. Abbreviations: RBP2, retinoblastoma binding protein 2; *RBP2* Mt, mutant demethylase *RBP2*; *RBP2* Wt, wild-type human *RBP2*.

RUNX2 to repress osteogenic differentiation of hASCs. To characterize the function of RBP2 in osteogenic differentiation of hASCs, a combination of in vitro experiments were carried out. By testing ALP activity, matrix mineralization capacity, and osteogenic gene expression profiles, which are common methods used in osteogenic differentiation studies, we found that *RBP2* depletion could promote osteogenic differentiation of hASCs via regulation of osteogenic associated genes. These preliminary observations are consistent with the current

understanding of the repression effect of *RBP2* in embryonic stem cell differentiation [24].

To solidify our observations in vivo, Bio-Oss Collagen transplantation was used to identify the role of RBP2 in an athymic mice xenograft model. Bio-Oss Collagen is a combination of purified cancellous natural bone mineral granules (Bio-Oss) and 10% collagen fibers in a block form and is sterilized by γ -irradiation. The collagen facilitates handling of the graft particles and acts to hold the Bio-Oss Collagen at the desired place. It acts as a framework onto which bone-forming cells and blood

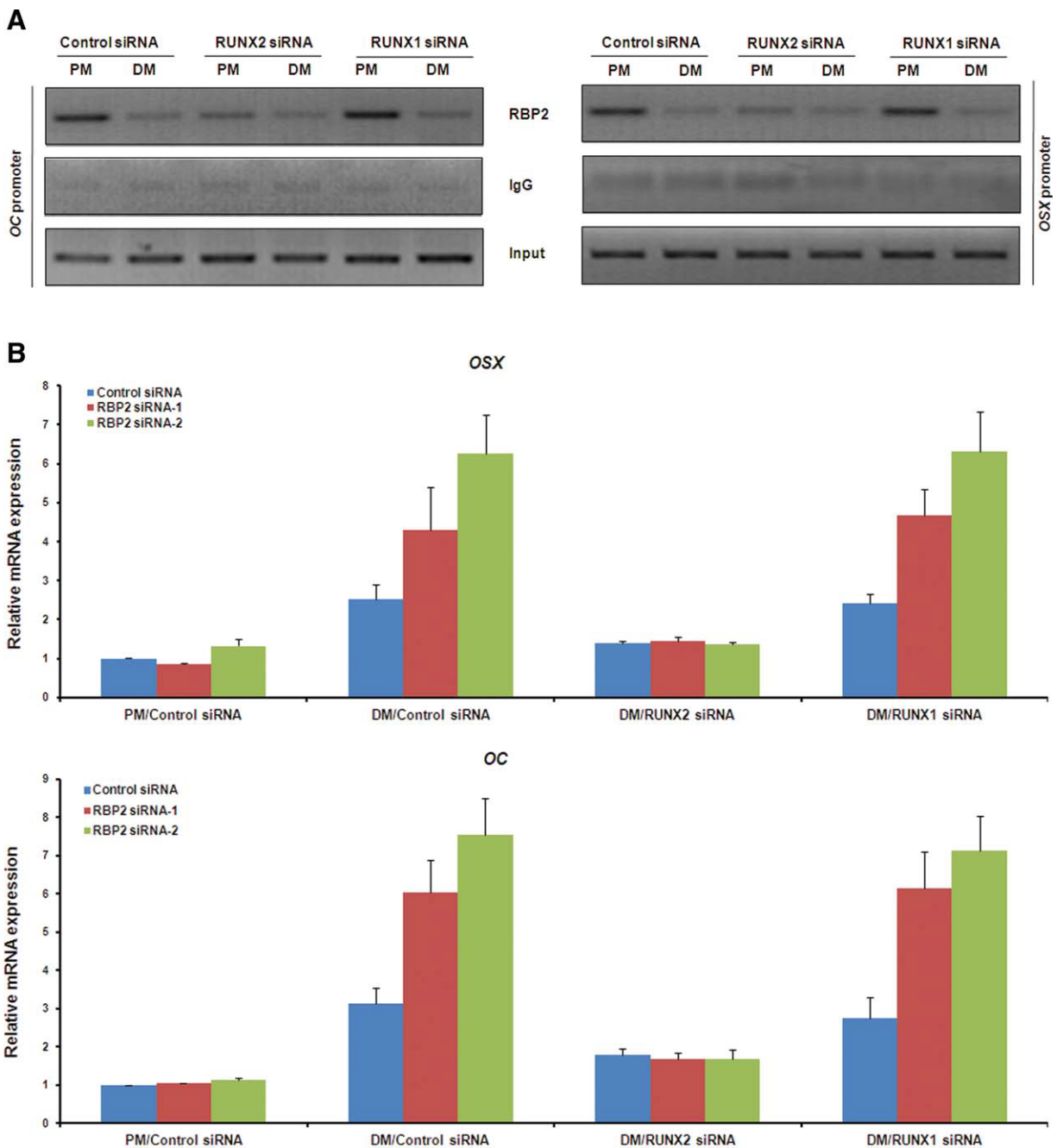


Figure 6. Loss of function of *RUNX2* impairs the repressive effect of retinoblastoma binding protein 2 (RBP2). **(A):** Human adipose-derived stromal cells (hASCs) were infected with control siRNA, *RUNX1* siRNA, or *RUNX2* siRNA lentivirus. Cells were cultured in proliferation or differentiation medium for 14 days. Soluble chromatin was prepared, and chromatin immunoprecipitation assays were performed with antibodies against the indicated proteins. **(B):** *RBP2* depleted hASCs were infected with control siRNA, *RUNX1* siRNA, or *RUNX2* siRNA lentivirus. Total RNAs were extracted from the cells for measurement of the mRNA expression of the indicated genes by real-time polymerase chain reaction (RT-PCR) normalized by *GAPDH* expression. Each bar represents the mean \pm SD of triplicate experiments. **(C):** Cellular extracts from the cells with the same treatment as in **(B)** were prepared to quantify alkaline phosphatase activity. Each bar represents the mean \pm SD of triplicate experiments. **(D):** The knockdown effects for *RBP2* (left panel), *RUNX1*, and *RUNX2* (right panel) were validated by RT-PCR normalized by *GAPDH* expression. Each bar represents the mean \pm SD of triplicate experiments. Abbreviations: *ALP*, alkaline phosphatase; DM, osteogenic differentiation medium; OC, osteocalcin; *OPN*, osteopontin; *OSX*, osterix; PM, proliferation medium; RBP2, retinoblastoma binding protein 2; siRNA, small interfering RNA.

vessels travel for formation of new bone. Bio-Oss Collagen has been reported to be highly osteoconductive [30]. Taking advantage of this system, we substantiated the function of RBP2 in vivo using x-ray imaging as well as histological and immunological staining. Furthermore, cell fates of hASCs in the scaffolds

were tracked by GFP signals contained in these lentivirus-infected cells. The LentiLox3.7 (pLL3.7) vector we used to encode *RBP2* siRNA has an independent EGFP cassette. The EGFP protein not only enables us to evaluate the lentivirus titration but also makes it possible to track the cell fate in osteogenic

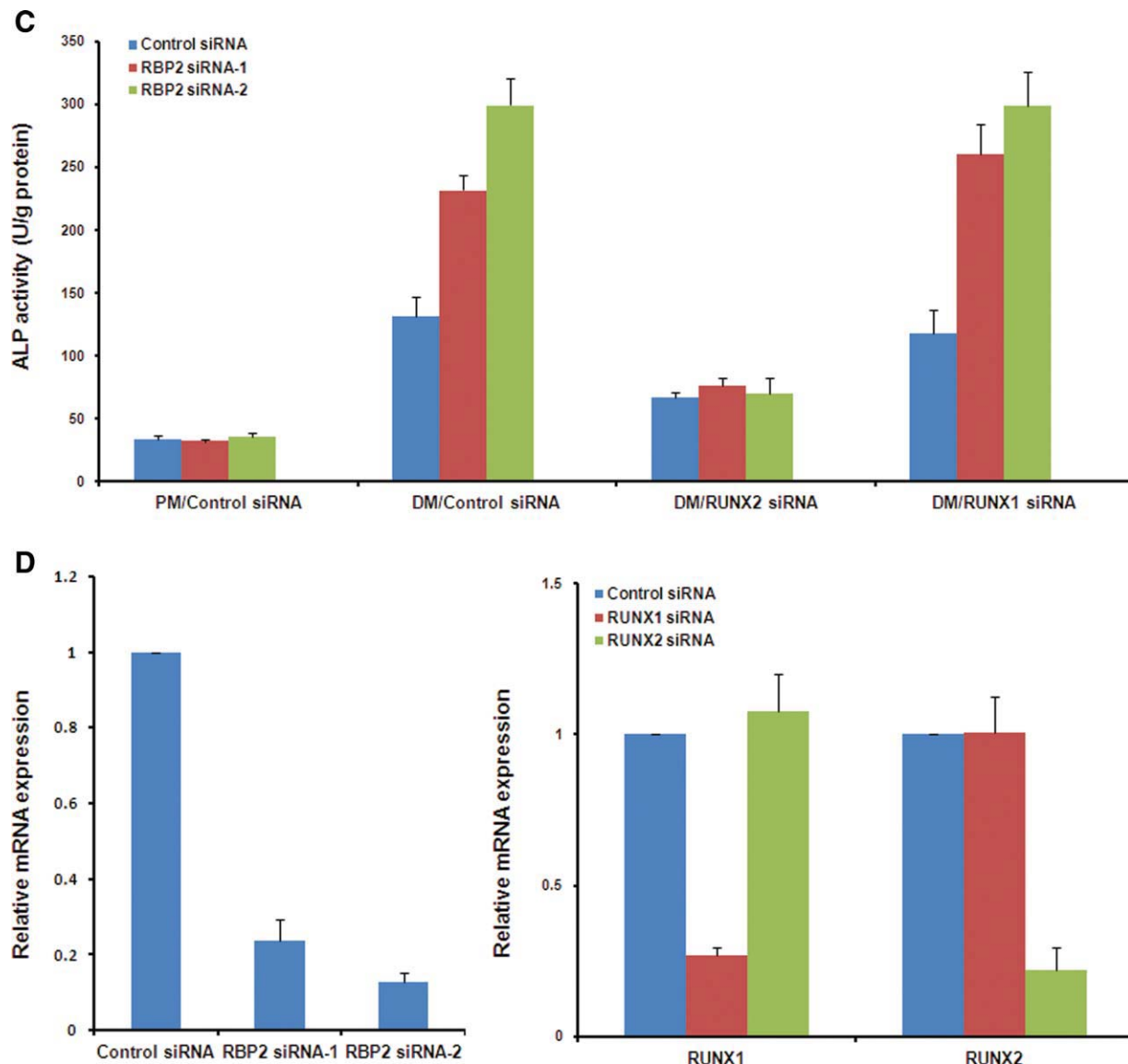


Figure 6. Continued

differentiation of hASCs. Taking this advantage, we checked the GFP signals by fluorescence microscope. The results demonstrated that the bone-forming cells still showed remarkable GFP signals (Supporting Information Fig. 1), indicating that these cells are derived from live hASCs carrying lentivirus.

Given the essential function of RUNX2 in activating a large repertoire of genes in osteogenesis, our data strongly suggested that RBP2 had a major role in osteogenic differentiation and function, adding a new layer of control in the regulation of the epigenetic program of osteogenesis. Our results further emphasized the idea that chromatin modification events were crucial for the control of RUNX2 function.

RUNX2 is an important osteoblast lineage-determining transcription factor involved in directing osteoblastic differentiation, and *RUNX2* appears to be the master gene for osteogenesis as it induces the expression of *OC*, *OSX*, bone sialoprotein, and *OPN*, which are required to finalize terminal osteoblast differentiation [31–33]. Although several studies have revealed that the recruitment of coactivators and corepressors is the likely mechanism underlying RUNX2-mediated

transcriptional regulation, it remains unclear how RUNX2 transcriptional activity is controlled during osteogenesis. To exert transcriptional repression at certain stages of osteogenesis, RUNX2 can associate with several corepressors, including mSin3A and histone deacetylases (HDACs) [34–38]. RBP2 is a lysine-specific histone demethylase that specifically removes H3K4me2 and H3K4me3 marks. The recruitment of RBP2 by RUNX2 suggested that the H3K4 histone demethylase activity of RBP2 in part conferred the repressive activity of RUNX2 and may have contributed to RUNX2-induced osteogenesis. This idea was further supported by the observations that *RBP2* loss of function promoted osteogenic differentiation of hASCs and that Wt RBP2 but not Mt RBP2 could repress RUNX2 transcriptional activity.

The negative regulation of RUNX2 activity by RBP2 in transient expression experiments required both physical interactions between RUNX2 and RBP2 as well as the demethylase activity of RBP2. Although the inhibition of the transcriptional activity of RUNX2 may certainly have been due to demethylation of histone H3, it could possibly also be caused

by demethylation of proteins that formed a complex with RUNX2 at the *OSX* and *OC* promoters or even by demethylation of RUNX2 itself. Previous evidence by others have shown that lysine-specific demethylase 1 (LSD1) demethylates K370me2 in p53 to regulate its activity [39], and we will explore this issue in our future investigations. As RBP2 did not affect the activation of an estrogen responsive element-driven luciferase reporter or *p21* promoter driven luciferase reporter (data not shown), the inhibition of RUNX2 activity by RBP2 in transient transfection experiments was highly specific, which we attributed to the direct interaction between RUNX2 and RBP2.

Despite the stable cellular levels of RBP2 after osteogenic induction (Fig. 1A), the occupancy of RBP2 at the endogenous *OSX* and *OC* promoters decreased (Fig. 4B). Furthermore, *RUNX2* depletion impaired RBP2 occupancy in native hASCs (Fig. 6A). From the above results, we propose a hypothetical regulation model. RBP2 or RBP2 containing repression complex is recruited by RUNX2 to the promoter regions of osteogenic genes (i.e., *OSX* and *OC*), which results in H3K4 demethylation at those promoters to inhibit expression of genes and maintain the undifferentiated state. However, in the proliferation medium, we found that the H3K4me3 mark remained at constantly low levels even when RBP2 was depleted. Emerging evidence suggests that in the absence of differentiation signals, osteogenic associated gene promoters are occupied by an assembly of transcription repressors such as HDACs, transducin-like enhancer of split proteins, mSin3A, and Yes-associated protein recruited by RUNX2 [35, 36, 40]. Depletion of *RBP2* itself may not recruit histone H3K4 methyltransferase and activate *OSX* and *OC* genes without recruitment of the differentiation induced activation complex. It is reasonable to speculate that other chromatin associated repressors may exert a compensatory transcription inhibition effect. When osteogenic differentiation is induced, RBP2 and the other possible repression complexes dissociate, and promoters of osteogenic genes become more accessible and occupied by activation complexes involving histone methylation or acetylation. Thus, the chromatin is altered from a repressed to an active state, although the exact mechanism by which this occurs is still unknown.

RBP2 belongs to the JmjC-domain subfamily and harbors functional motifs including Plant Homeo Domain and Bright/Arid domains, which are found in many proteins associated with chromatin and transcriptional regulation [41–46].

Additional studies will need to delineate domains in RBP2 that mediate such interactions with RUNX2 in the future.

In summary, our results demonstrated for the first time that RBP2 inhibits osteogenic differentiation of hASCs by repression of RUNX2-activated transcription. Our observations not only support the functional role of RBP2 in osteogenic differentiation but also contribute to further understanding of the epigenetic layer of RUNX2-activated gene transcription. To some extent, we also provide valuable information on how to promote osteogenic differentiation of hASCs for the bone tissue engineering field. It may be possible and highly beneficial to develop tissue selective RBP2 inhibitors that can change epigenetic characteristics of hASCs or other types of stem cells for epigenetic therapy, which have paid off in the treatment of cancer [47, 48].

CONCLUSION

Our investigations of the functional role and mechanism of the H3K4 demethylase RBP2 in osteogenic differentiation of hASCs demonstrated that RBP2 inhibited osteogenic differentiation of hASCs in vitro and in vivo. It occupied osteogenesis-associated genes *OSX* and *OC* promoters to maintain the level of H3K4me3. RBP2 could interact with RUNX2 and repress the transcriptional activity of RUNX2 through its H3K4 demethylase activity. Furthermore, we report that inhibition of osteogenic differentiation of hASCs by RBP2 was dependent on RUNX2.

ACKNOWLEDGMENTS

We thank Dr. Shenglin Li (Core Laboratory, Peking University School of Stomatology, Beijing, China) for her technical supports. This study was supported by a grant from the National Natural Science Foundation of China (No. 81070809).

DISCLOSURE OF POTENTIAL CONFLICTS OF INTEREST

The authors indicate no potential conflicts of interest.

REFERENCES

- Zuk PA, Zhu M, Ashjian P et al. Human adipose tissue is a source of multipotent stem cells. *Mol Biol Cell* 2002;13:4279–4295.
- Tapp H, Hanley EN, Jr, Patt JC et al. Adipose-derived stem cells: Characterization and current application in orthopaedic tissue repair. *Exp Biol Med (Maywood)* 2009;234:1–9.
- Rada T, Reis RL, Gomes ME. Adipose tissue-derived stem cells and their application in bone and cartilage tissue engineering. *Tissue Eng Part B Rev* 2009;15:113–125.
- Bosnakovski D, Mizuno M, Kim G et al. Isolation and multilineage differentiation of bovine bone marrow mesenchymal stem cells. *Cell Tissue Res* 2005;319:243–253.
- Zhou Y, Ni Y, Liu Y et al. The role of simvastatin in the osteogenesis of injectable tissue-engineered bone based on human adipose-derived stromal cells and platelet-rich plasma. *Biomaterials* 2010;31:5325–5335.
- Levi B, James AW, Wan DC et al. Regulation of human adipose-derived stromal cell osteogenic differentiation by insulin-like growth factor-1 and platelet-derived growth factor-alpha. *Plast Reconstr Surg* 2010;126:41–52.
- Liu Y, Zhou Y, Feng H et al. Injectable tissue-engineered bone composed of human adipose-derived stromal cells and platelet-rich plasma. *Biomaterials* 2008;29:3338–3345.
- Lee SJ, Kang SW, Do HJ et al. Enhancement of bone regeneration by gene delivery of BMP2/Runx2 bicistronic vector into adipose-derived stromal cells. *Biomaterials* 2010;31:5652–5659.
- Dragoo JL, Lieberman JR, Lee RS et al. Tissue-engineered bone from BMP-2-transduced stem cells derived from human fat. *Plast Reconstr Surg* 2005;115:1665–1673.
- Doi A, Park IH, Wen B et al. Differential methylation of tissue- and cancer-specific CpG island shores distinguishes human induced pluripotent stem cells, embryonic stem cells and fibroblasts. *Nat Genet* 2009;41:1350–1353.
- Boquest AC, Noer A, Sorensen AL et al. CpG methylation profiles of endothelial cell-specific gene promoter regions in adipose tissue stem cells suggest limited differentiation potential toward the endothelial cell lineage. *Stem Cells* 2007;25:852–861.
- Boquest AC, Noer A, Collas P. Epigenetic programming of mesenchymal stem cells from human adipose tissue. *Stem Cell Rev* 2006;2:319–329.
- Adams-Cioaba MA, Min J. Structure and function of histone methylation binding proteins. *Biochem Cell Biol* 2009;87:93–105.
- Pasini D, Malatesta M, Jung HR et al. Characterization of an antagonistic switch between histone H3 lysine 27 methylation and

- acetylation in the transcriptional regulation of Polycomb group target genes. *Nucleic Acids Res* 2010;38:4958–4969.
- 15 Dahl JA, Reiner AH, Klungland A et al. Histone H3 lysine 27 methylation asymmetry on developmentally-regulated promoters distinguish the first two lineages in mouse preimplantation embryos. *PLoS One* 2010;5:e9150.
 - 16 Shi Y, Lan F, Matson C et al. Histone demethylation mediated by the nuclear amine oxidase homolog LSD1. *Cell* 2004;119:941–953.
 - 17 Cloos PA, Christensen J, Agger K et al. Erasing the methyl mark: Histone demethylases at the center of cellular differentiation and disease. *Genes Dev* 2008;22:1115–1140.
 - 18 Klose RJ, Yamane K, Bae Y et al. The transcriptional repressor JHDM3A demethylates trimethyl histone H3 lysine 9 and lysine 36. *Nature* 2006;442:312–316.
 - 19 Tsukada Y, Fang J, Erdjument-Bromage H et al. Histone demethylation by a family of JmjC domain-containing proteins. *Nature* 2006;439:811–816.
 - 20 Shi Y, Whetstine JR. Dynamic regulation of histone lysine methylation by demethylases. *Mol Cell* 2007;25:1–14.
 - 21 Klose RJ, Zhang Y. Regulation of histone methylation by demethylination and demethylation. *Nat Rev Mol Cell Biol* 2007;8:307–318.
 - 22 Christensen J, Agger K, Cloos PA et al. RBP2 belongs to a family of demethylases, specific for tri- and dimethylated lysine 4 on histone 3. *Cell* 2007;128:1063–1076.
 - 23 Klose RJ, Yan Q, Tothova Z et al. The retinoblastoma binding protein RBP2 is an H3K4 demethylase. *Cell* 2007;128:889–900.
 - 24 Pasini D, Hansen KH, Christensen J et al. Coordinated regulation of transcriptional repression by the RBP2 H3K4 demethylase and Polycomb-Repressive Complex 2. *Genes Dev* 2008;22:1345–1355.
 - 25 Benevolenskaya EV, Murray HL, Branton P et al. Binding of pRB to the PHD protein RBP2 promotes cellular differentiation. *Mol Cell* 2005;18:623–635.
 - 26 Shang Y, Hu X, DiRenzo J et al. Cofactor dynamics and sufficiency in estrogen receptor-regulated transcription. *Cell* 2000;103:843–852.
 - 27 Shang Y, Brown M. Molecular determinants for the tissue specificity of SERMs. *Science* 2002;295:2465–2468.
 - 28 Whetstine JR, Nottke A, Lan F et al. Reversal of histone lysine trimethylation by the JMJD2 family of histone demethylases. *Cell* 2006;125:467–481.
 - 29 Fodor BD, Kubicek S, Yonezawa M et al. Jmjd2b antagonizes H3K9 trimethylation at pericentric heterochromatin in mammalian cells. *Genes Dev* 2006;20:1557–1562.
 - 30 Wong RW, Rabie AB. Effect of bio-oss collagen and collagen matrix on bone formation. *Open Biomed Eng J* 2010;4:71–76.
 - 31 Komori T. Regulation of bone development and maintenance by Runx2. *Front Biosci* 2008;13:898–903.
 - 32 Komori T. Runx2, a multifunctional transcription factor in skeletal development. *J Cell Biochem* 2002;87:1–8.
 - 33 Komori T. Requisite roles of Runx2 and Cbfb in skeletal development. *J Bone Miner Metab* 2003;21:193–197.
 - 34 Schroeder TM, Kahler RA, Li X et al. Histone deacetylase 3 interacts with runx2 to repress the osteocalcin promoter and regulate osteoblast differentiation. *J Biol Chem* 2004;279:41998–42007.
 - 35 Westendorf JJ. Transcriptional co-repressors of Runx2. *J Cell Biochem* 2006;98:54–64.
 - 36 Lamour V, Detry C, Sanchez C et al. Runx2- and histone deacetylase 3-mediated repression is relieved in differentiating human osteoblast cells to allow high bone sialoprotein expression. *J Biol Chem* 2007;282:36240–36249.
 - 37 Sun X, Wei L, Chen Q et al. HDAC4 represses vascular endothelial growth factor expression in chondrosarcoma by modulating RUNX2 activity. *J Biol Chem* 2009;284:21881–21890.
 - 38 Jensen ED, Schroeder TM, Bailey J et al. Histone deacetylase 7 associates with Runx2 and represses its activity during osteoblast maturation in a deacetylation-independent manner. *J Bone Miner Res* 2008;23:361–372.
 - 39 Huang J, Sengupta R, Espejo AB et al. p53 is regulated by the lysine demethylase LSD1. *Nature* 2007;449:105–108.
 - 40 Jensen ED, Nair AK, Westendorf JJ. Histone deacetylase co-repressor complex control of Runx2 and bone formation. *Crit Rev Eukaryot Gene Expr* 2007;17:187–196.
 - 41 Chen Z, Zang J, Kappler J et al. Structural basis of the recognition of a methylated histone tail by JMJD2A. *Proc Natl Acad Sci USA* 2007;104:10818–10823.
 - 42 Couture JF, Collazo E, Ortiz-Tello PA et al. Specificity and mechanism of JMJD2A, a trimethyllysine-specific histone demethylase. *Nat Struct Mol Biol* 2007;14:689–695.
 - 43 Huang Y, Fang J, Bedford MT et al. Recognition of histone H3 lysine-4 methylation by the double tudor domain of JMJD2A. *Science* 2006;312:748–751.
 - 44 Lee J, Thompson JR, Botuyan MV et al. Distinct binding modes specify the recognition of methylated histones H3K4 and H4K20 by JMJD2A-tudor. *Nat Struct Mol Biol* 2008;15:109–111.
 - 45 Ng SS, Kavanagh KL, McDonough MA et al. Crystal structures of histone demethylase JMJD2A reveal basis for substrate specificity. *Nature* 2007;448:87–91.
 - 46 Shi X, Hong T, Walter KL et al. ING2 PHD domain links histone H3 lysine 4 methylation to active gene repression. *Nature* 2006;442:96–99.
 - 47 Catalano MG, Poli R, Pugliese M et al. Emerging molecular therapies of advanced thyroid cancer. *Mol Aspects Med* 2010;31:215–226.
 - 48 Hodges SJ, Yoo JJ, Mishra N et al. The effect of epigenetic therapy on congenital neurogenic bladders—A pilot study. *Urology* 2010;75:868–872.



See www.StemCells.com for supporting information available online.